Available online at www.sciencedirect.com
SCIENCE DIRECT®
CARBOHYDRATE RESEARCH
ELSEVIER
Carbohydrate Research 338 (2003) 2459–2475
www.elsevier.com/locate/carres

Perspective/Review

Characterisation of bacterial polysaccharides: steps towards single-molecular studies

Marit Sletmoen,[a,†] Gjertrud Maurstad,[a,†] Pawel Sikorski,[a] Berit Smestad Paulsen,[b] Bjørn T. Stokke[a,*]

[a] *Biophysics and Medical Technology, Department of Physics, The Norwegian University of Science and Technology, NTNU, NO-7491 Trondheim, Norway*

[b] *Department of Pharmacognosy, School of Pharmacy, University of Oslo, P.O. Box 1068 Blindern, NO-0316 Oslo, Norway*

Received 15 April 2003; accepted 24 July 2003

Abstract

Techniques used in studies of polysaccharides, including chemical composition, linkage pattern, and higher order structures are in constant development. They provide information necessary for understanding of the polysaccharide properties and functions. Here, recent advancements in studies of the polysaccharides at the single-molecule level are highlighted. Over the last few years, single-molecule techniques such as force spectroscopy have improved in sensitivity and can today be used to detect forces in the pN range. In addition, these techniques can be used to investigate properties of single molecules close to physiological conditions. The challenges in the interpretation of the observations are aided by control experiments using well-characterised polysaccharides and by data provided by complementary methods. This field is expected to have increasing impact on the further advancement of the molecular understanding of the role of polysaccharides in various biological processes such as recognition and cell adhesion.

Keywords: X-ray fibre diffraction; AFM; TEM; Force spectroscopy; Single-molecules

Contents

* Corresponding author. Fax: +47-73-597-710.
E-mail address: bjorn.stokke@phys.ntnu.no (B.T. Stokke).
† These authors have contributed equally to the work.

0008-6215/03/$ - see front matter © 2003 Elsevier Ltd. All rights reserved.
doi:10.1016/j.carres.2003.07.007

1. Introduction

Polysaccharides serve many important functions in nature, such as building a mechanically strong structure, storing energy in a readily accessible form and ensuring specificity in biological recognition and communication. A molecular understanding of the various functions relies on insight into the detailed structure of these materials. The structural information includes description of the chemical composition and geometric arrangements of the atoms and molecules at various length scales. To this end, an arsenal of methods has been developed over the years. The general trend in the development of such techniques is an increase in sensitivity, an expansion of the measurable size range, and a tendency to move closer to the biologically relevant state. Here we focus on a set of techniques that has the potential to provide increased insight into the main features underlying the functions of polysaccharides while at the same time allowing application closer to the native environment (Fig. 1). Additionally, this captures important current trends in the development of techniques or the application of these in a novel way, for determination of properties of polysaccharides.

We start with a brief description of methods for primary structure determination. This information is needed in the interpretation of diffraction patterns of fibrous samples, which additionally provide information about preferred conformations expressed in terms of torsional angles ϕ, ψ, and ω in the glycosidic linkages. Additionally, fibre diffraction yields structural information about higher order structural elements such as helicity and the number of carbohydrate chains forming intertwining helices. Ultramicroscopic techniques such as transmission electron microscopy (TEM) and the later developed scanning probe microscopes, in particular atomic force microscopy (AFM), allow determination of single-molecule properties. This is so in imaging mode where manifestations of thermally agitated fluctuations around the preferred conformations can be directly visualised and eventual helical structure can be deduced indirectly or seen directly. Additionally, AFM can be used to stretch single polysaccharide chains allowing the determination of mechanical fingerprints reflecting the chemical composition, linkage geometry and higher order structure. Such single molecule probe techniques can also be applied for direct determination of molecular interactions, which is a prerequisite for e.g. cell signalling, or interactions between polysaccharides (like and unlike) in general. In such a way, the information from these various techniques merges into a comprehensive description that provides a fundament for understanding the function of polysaccharides.

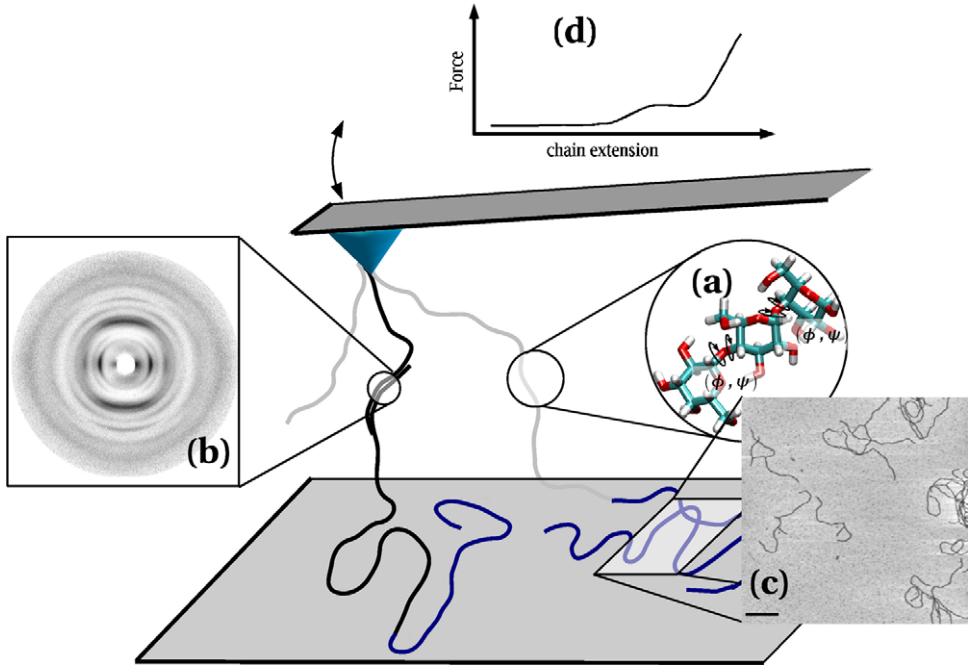

Fig. 1. Schematic illustration of how information obtained from a selection of experimental techniques is coupled together in order to describe polysaccharides at different length scales. The methods described in this article include: a combination of chemical characterisation and conformational analysis (a); scattering techniques (e.g., fibre X-ray diffraction from crystalline molecular assemblies) (b); imaging by TEM and AFM (c); interaction studies with the use of AFM as a force measuring instrument (d). The torsional angles of the glycosidic bond, in addition to ϕ and ψ, cen include ω, e.g., for (1→6)-linkages. (Reprinted from Carbohydrate Research, Vol. 252, Lee et al., Structural roles of calcium ions and side chains in welan: an X-ray study, pp. 183–207, Copyright 1994, with permission from Elsevier.)

The examples included in the following are mostly bacterial polysaccharides. However, additional polysaccharides are discussed either as necessary model compounds, or because they have been studied using approaches considered applicable to bacterial polysaccharides. In addition to the techniques discussed, there have been advances in the development of other physical characterisation techniques. These include e.g. scattering techniques such as small-angle X-ray scattering[1] and dynamic light scattering for characterisation of non-ergodic states and turbid systems, NMR techniques for investigation of e.g. sequence and conformational properties, and various approaches for determination of size. Where appropriate complementary results have been or could have been obtained by such techniques, they will be referred to.

2. Primary structure

2.1. Structural variability in bacterial polysaccharides

The primary structure of proteins and polysaccharides describes the arrangement of the different building blocks, amino acids and monosaccharides respectively, along the polymer chain. The possible structural variability due to available units and connecting patterns is estimated to be about three orders of magnitude larger for polysaccharides than for proteins.[2] Moreover, since the primary structure of polysaccharides is not coded directly in the genetic sequence, the advancement in primary structure determination has not evolved as rapidly within the polysaccharide field as it has for proteins. This, together with the fact that the experimental procedures for determination of the relative contents and arrangement of the monosaccharides are technically more demanding, makes the description of the polysaccharide primary structure not an easy task.

2.2. Determination of monosaccharide composition

Determination of the overall monosaccharide composition of polysaccharides often requires cleavage of all the glycosidic linkages in the polysaccharide by acid hydrolysis. Differences in hydrolysis kinetics as well as degradation of released monosaccharides offer complications to the experimental protocols. Nevertheless, this procedure has been used successfully in a number of studies, a recent example being the hydrolysis of pneumococcal polysaccharides reported by Talaga and co-workers.[3] Bacterial polysaccharides are special in the sense that they have a repeated structural motif with 2–8 sugar residues, the sequence of which can be determined by NMR. Currently known exceptions from this include bacterial alginates. Procedures involving cleavage of the glycosidic bonds are not always needed in order to determine the monosaccharide composition. In some cases the sequence of the repeated unit cannot be determined unambiguously from NMR spectra of the intact polymers, due to poor resolution in the resulting spectra. In such cases, more reliable structural information can be obtained from studies of oligosaccharide samples. Oligosaccharide fragments can be prepared from the polysaccharide either by mild acid hydrolysis or enzymatic degradation with specific enzymes. One example is the use of NMR and MS in combination for the structural determination of the O-specific polysaccharide of *Vibrio cholerae* O8.[4]

NMR studies can also provide information about the stereochemical configuration, especially the anomeric configuration, of the monomers in the polymer chains.[5] In general, when obtaining spectra from higher molecular weight oligosaccharides and polymers, the characteristic signals from the end residues diminishes and finally disappears when the molecular weight exceeds a certain limit. The anomeric configuration is therefore easier to determine from NMR spectra of short fragments.

Different types of chromatographic methods can be used for isolation of the oligosaccharides. Fractions containing only oligosaccharides of a certain length can be isolated and subjected to further analysis. One elegant separation procedure is High Performance Anion Exchange Chromatography coupled with a Pulse Amperometric Detector (HPAEC-PAD) as described by Brüll et al.[6] The purified oligomers can be subjected to further analyses by desorption and ionisation methods like fast atom bombardment (FAB), electrospray ionization (ESI), or matrix assisted laser desorption ionization (MALDI) coupled to MS.[7] Such soft ionisation methods will in most cases give rise to ions of the intact oligomers and their fragments, resulting in mass spectra from which an overall information on the sequence of the monomers can be deduced. Tandem MS is a powerful technique in this respect that allows determination of complex sequences. For bacterial polysaccharides, the results of the MS experiments coupled with methylation studies of the oligomers formed can lead to the sequence of the repeating unit. For example, an extracellular polysaccharide produced by the cyanobacterium *Nostoc commune* has been studied using this approach.[6] Oligomers up to five units were separated and identified. It was also found by this method that certain units in the polysaccharide had one of the glucose units methylated at position 2.

2.3. Determination of linkage geometry, monosaccharide configuration and substituent decoration

Chemical determination of the type of linkages between the monomers is best performed by gas-chromatography coupled with mass spectrometry (GC–MS) analysis of

the partially methylated, alditol acetates obtained after a complete methylation of the polymer followed by acid hydrolysis, reduction and acetylation. Monosaccharides exist both in the D- and L-configuration. Hexoses are normally present as D-sugars, but other monosaccharides, e.g., arabinose, rhamnose and fucose, have a tendency to exist in the L-sugar form. The absolute configuration can be determined by GC of glycosides prepared using an optical active alcohol, e.g., (+)-2-butanol, basically according to the method described by Gerwig et al.[8] The configuration of the monosaccharides is determined by comparing the results of GC analysis of the (+)-2-butyl glycosides TMS-ethers, with those of references.

Bacterial polysaccharides may also contain other components than monosaccharides; methyl ether groups may be present on all possible positions,[6] and decorations with acetate, sulfate and pyruvate esters are also found. The position of the substituents can be determined e.g., by IR or NMR, or by GC–MS analysis of derived alditol acetates obtained after complete hydrolysis of the polymers.

3. Molecular structure

3.1. Information obtainable from X-ray diffraction studies of polysaccharides

Fibre X-ray diffraction studies is the preferred method for establishing the three-dimensional structure and organisation of long chain polymers and biopolymers.[9] So far, for these compounds it has not been possible to grow single crystals sufficiently large to allow studies by single-crystal diffraction techniques. To our knowledge, the longest polysaccharide fragment studied by single crystal X-ray diffraction is cycloamylose, with 26 glucose residues.[10] Oriented polycrystalline fibre patterns, however, can usually provide the information required to establish the conformation of the polymer chains, describe the lateral packing, and sometimes even allow the determination of the co-ordinates of ions included within the structure.[11] The information needed to fully describe the shape and structure of a polysaccharide chain can be divided into three groups. The ring conformation for each of the units in the chemical repeat must first be described, then the relative orientation of adjacent saccharide units must be characterised, and finally questions related to the possible formation of intertwining helices and the orientation of the polymer chains (parallel, antiparallel) should be addressed. The relative orientation of the adjacent saccharide units is usually expressed in terms of the torsion angles ϕ, ψ, and ω around the glycosidic bond (Fig. 1a). Often, molecular models are used to find the (ϕ, ψ, ω) values which satisfy the constraints imposed by the experimental data. For example, the pitch and the symmetry of a helix formed by the polysaccharide chain can be deduced from X-ray diffraction studies of fibres. In addition, information about the distribution of ϕ, ψ, ω torsion angles for a particular polysaccharide can be determined from solution NMR measurements,[12,13] or from molecular modelling.

In general, the fibre diffraction pattern bears a resemblance to that from a rotating single crystal. In fibres, crystallites are aligned in such a way that the polymer chain axis (typically c-axis) runs parallel to the axis of the fibre. The azimuthal orientation of the crystallites is random. A diffraction pattern taken with the X-ray beam orthogonal to the fibre axis is therefore similar to a single crystal rotation pattern, with the crystal being rotated about c by 360°. In this type of pattern, all the hkl diffraction intensities can be recorded nearly simultaneously. For an orthorhombic or a monoclinic unit cell, the diffracted intensities are located on a set of parallel (if the film has a cylindrical shape) or hyperbolic (for a flat film) layer lines. The a^* and b^* directions ($hk0$ diffraction signals) are located on the equator and c^* is parallel to the meridian. The spacing between the layer lines, for the flat film case measured on the meridian, represents the stereochemical repeat distance along the polymer chain direction. This repeat usually includes more than one chemical unit. Furthermore, for a chain in a helical conformation with n = number of units in a single turn, the diffracted intensities on the meridian only occurs for the layer lines with index l which is a multiple of n. For example, for a 5_1 helix meridional reflections will occur on the 5th and the 10th layer lines.

In addition, the systematic absence of diffracted intensities on entire layer lines provides information on whether the polymer chains form single, double or triple helixes. For example, in the case of two chains forming an intertwining double helix, all odd layer lines will be missing. Additionally, a small disruption of the perfect double helix, caused by for example changes in the relative humidity, can bring up weak intensities on the missing layer lines. This fact can therefore be used to further validate a double helical model.

In the structure determination procedure, the density of the crystalline fibres should also be determined experimentally (e.g., by the flotation method). This is useful for two reasons, the first being that it can help establishing the number of polymer chains per unit cell and the amount of hydration water. Secondly, large differences between the measured density and the density calculated from the unit cell volume can indicate errors in the assignment of the indexes to the diffraction signals and as a consequence errors in the determined unit cell parameters.

A more detailed analysis of the diffraction intensities is needed in order to determine atomic co-ordinates,

positions of ions involved in interchain interactions, etc. In the most commonly used structure determination procedure, the initial structural data is used to build a starting model, which is then refined against observed diffraction intensities and stereochemical interactions.

Finally, we should mention that even in the case of high resolution X-ray diffraction data, it is usually not possible to the determine positions of the hydrogen atom with confidence. This is due to the fact that hydrogen is a relatively weak scatterer of X-rays. It is however a strong scatterer of neutrons. Neutrons are also scattered in a significantly different way by different isotopes of hydrogen. The power of neutron diffraction in combination with specific deuteration for locating hydrogen atoms and water molecules has recently been shown in studies of cellulose[14–17] and other biopolymers.[18] In one example, Nishiyama et al.[16] used a combination of fibre X-ray and neutron diffraction to study the crystal structure and hydrogen-bonding system in cellulose Iβ. The data was recorded for oriented fibrous samples prepared by aligning cellulose microcrystals from tunicin. The X-ray data were used to determine the C and O atom positions. The positions of the hydrogen atoms involved in hydrogen bonding were determined from a Fourier-difference analysis using neutron diffraction data collected from non-deuterated and deuterated samples. It was discovered that the hydrogen atoms involved in the intramolecular hydrogen bonds between O3 and O5 have well-defined positions. On the other hand, the diffraction data and IR observations indicated an intrinsic disorganization of the hydrogen bond pattern for O-2 and O-6, suggesting multiple geometry with partial occupation.

Stable associations between polysaccharide chains in the solid state are believed to bear a similarity to the associations of the polymer chains involved in formation of junction zones in polysaccharide gels. Understanding the junction zone structure is a critical step towards identifying factors important in gel formation. The structure in the solid state can also reveal the preferred conformations of the polysaccharide chain. For example, it was discovered for poly α-L-guluronic acid that the shape of the molecule could both provide insight into how the polymers interact with each other and identify factors important for this process. Fibre X-ray diffraction studies showed that the guluronic acid unit is in the $^{1}C_{4}$ conformation, giving the polymer chain a characteristic zigzag appearance.[19] This discovery was a critical step in describing the mechanism of junction zone formation involving divalent cations (so called egg-box model).[20]

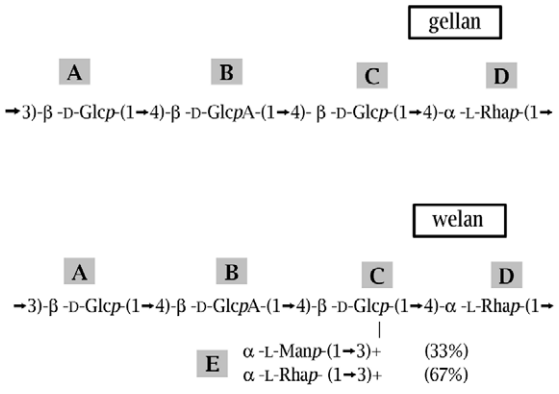

Fig. 2. Basic chemical structure of the repeat units of gellan (a) and welan (b) polysaccharides. The Glc*p* residue depicted **A** in native gellan is substituted at O-2 with L-glycerol and at O-6 with acetyl groups (50%).[101,102]

3.2. X-Ray diffraction studies of the bacterial polysaccharide welan

To illustrate how fibre X-ray diffraction can be used to study polysaccharides we will discuss welan, an industrially important bacterial polysaccharide from the gellan family. To do so, we should first briefly mention the structure and properties of gellan. It is a linear, ionic polysaccharide with a chemical repeat consisting of four units (ABCD, Fig. 2a). Native gellan includes approximately 6% by weight O-acyl groups, and under appropriate conditions it can form weak elastic gels.[21] In the solid state, gellan polymer chains form intertwining double-helical structures. The polymer chains are parallel, half-staggered (relative *c*-axis shift of *c*/2) and have a 3-fold conformation.[22] Weak gel formation is attributed to the interaction between double-helices and is influenced by the presence of monovalent or divalent cations.

Aqueous solutions of deacetylated gellan are very viscous and can form gels at concentrations as low as 0.04%. An important feature of gellan gels is their thermoreversibility.

Gellan was extensively used in the past as a model system for studying the mechanism of gelation of polysaccharides. Upon heating, the double-helical structure of native gellan can be thermally dissociated. In the older model for the gelation of gellan and related polysaccharides like κ-carrageenan, it was suggested that upon cooling some of the double helices would reform and thereby interconnect many different polymer chains. This process would lead to junction zones supporting connectivity in the network formation. Recent direct imaging studies using AFM indicate that the gels are formed by fibrous, ion-mediated aggregates of double-helices rather than by double helices connected by more flexible disordered chains.[23–25]

The main chain chemical repeat of welan share the four sugar units (ABCD, Fig. 2b) of gellan. In addition, welan has a side chain (E) of which approximately two thirds are α-L-rhamnopyranosyl and the remaining are α-L-mannopyranosyl units. Approximately 85% of the

3-linked glucosyl units (A) are substituted with O-acetyl groups in the 2-position.[26] Despite similarities in the chemical structure between welan and gellan, welan is a non gelling polysaccharide, forming highly viscous aqueous solutions which are stable up to 130 °C. Based on the fact that no thermally induced gelation is observed, Crescenzi et al.[27] postulated a model in which, in solution, welan polymer chains exist in a disordered coil structure, and do not form intertwining double-helices similar to that of gellan.

An attempt to visualise single welan polymer chains by TEM is shown in Fig. 3a. As expected, the observed objects are elongated, but much less flexible than what one would expect from the linkage pattern. The appearance of the polymer chains is similar to that seen for gellan double helices,[25,28,29] suggesting that welan forms similar structures. Extensive TEM investigations involving a variety of preparation conditions failed to produce welan chains in a more disordered conformation. Other studies showed that the solution properties of welan in aqueous solution are unaffected by heating (up to above 100 °C)[30,31] or cooling. However, changes similar to those observed for gellan can be induced if welan is dissolved in Me_2SO/water mixtures.[30,31]

The final proof of the double-helix structure of welan came from fibre X-ray diffraction. Oriented and highly crystalline fibres of welan calcium salt (see pattern reproduced in Fig. 3b) were studied by Chandrasekaran et al.[26] The interpretation of the diffraction data showed that the backbone conformation is similar to that observed for gellan. It was discovered that the side chains fold back on to the main chain, to form hydrogen bonds with the carboxylate groups. It was suggested that this feature have a strong stabilising effect on the double helix, providing an explanation why no thermally induced dissociation is observed in aqueous solution. However at temperatures as high as 100 °C and in aqueous environment, one would expect the conformation of the side chain to be highly disordered, with hydrogen bonds between the side chain, the main chain and the surrounding solvent dynamically breaking and forming. Therefore the side chain should only have a small effect on the stability of the double-helical structure at such high temperatures. An alternative explanation for the increased stability of the welan double-helix at elevated temperatures considers the contribution from the disordered side chain to the conformational entropy of the double helix. This contribution will lower the entropy difference between the ordered double helix state and the disordered single chain state. It therefore will have a stabilising effect raising the "melting" temperature of the double-helix. For certain, presence of this short side chains will hinder association of the double-helices, preventing formation of gels.

4. Imaging of bacterial polysaccharides by EM and AFM

While X-ray diffraction can be used for structure determination on the atomic scale, imaging by the ultramicroscopic techniques TEM and AFM provide information in the nm to μm range. These techniques can be used to determine, for example, the distribution of the polymer chain lengths, polymer chain flexibility (i.e., the persistence length, L_p) and the mass per unit length, M_L. Much of the information obtainable by TEM and AFM is similar, and therefore they will be discussed together. At first, however, we would like to point out some of the important differences between these two imaging techniques. Imaging with the use of TEM requires the sample being compatible with high vacuum. In many instances, TEM requires elaborated preparation procedures to achieve contrast enhancement and vacuum compatibility. The influence of

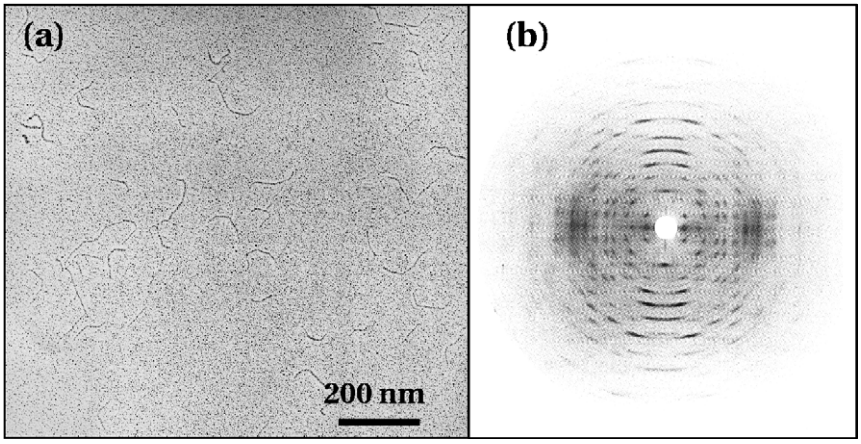

Fig. 3. Electron micrographs of welan gum (a) (unpublished work by the authors). Fibre X-ray diffraction pattern recorded from crystalline and well oriented fibres of welan calcium salt (b), reproduced with permission from Chandrasekaran et al.[26]

artefacts associated with the preparation procedure needs proper attention in order to avoid possible misinterpretations of the image. AFM has the advantage of offering an operating environment close to physiological conditions, with the images being recorded in air or when the sample is immersed in liquid, e.g., water.

4.1. Determination of polymer chain flexibility using EM and AFM

Ultramicroscopy provides direct pictorial evidence of chain flexibility reflecting the linkage pattern of the polysaccharide chains, e.g., (1→3), (1→4). In Fig. 4, electron micrographs and AFM topographs of some polysaccharides having different linkage patterns are shown. A bacterial exopolysaccharide produced by the halophilic Archaon *Haloferax mediterranei*[32] having mixed (1→6) and (1→4) linkages, the polysaccharide sclerox having a (1→3)-linked β-D-Glc*p* backbone,[33] and (1→4)-linked alginate[34] (fraction of guluronic acid, $F_G = 0.66$) are shown. Although the chain stiffness of polyelectrolytes is influenced by the ionic strength of the solution, the images show that the mixed (1→6), (1→4) linkages yield the most flexible structure. Additionally, a dramatic increase in chain stiffness is seen when comparing the double-stranded welan (Fig. 3a) with the individual chains having (1→4) or (1→3) linkages. This type of information can be used to study the correlation between flexibility and linkage geometry. The reverse problem, i.e., deducing the detailed linkage pattern from the observed tortuosity is, however, not currently possible because a similar appearance can be realised by different linkage patterns.

Parameters describing chain flexibility can be quantitatively determined from observed chain trajectories. One prerequisite for quantifying the chain stiffness from the chain trajectory is that the entire contour of individual molecules is visible, free from overlaps and distinguishable from the background. This limitation sets a lower bound on the flexibility of polymers that can be investigated using AFM and TEM. Polysaccharides that are more flexible than sclerox and alginate (Fig. 4; L_p in the range 5–20 nm), e.g., dextran ($L_p \sim 2$ nm [35]), have a globular appearance that does not allow assignment of chain trajectories.

The analysis of chain flexibility from observed chain trajectories requires adoption of a model. Generally, the micrographs depict macromolecular structures on a surface, for which either a two-, three- or intermediate dimensionality is an appropriate basis for the analysis.[36–39] A preparation procedure yielding an image as a projection of a 3D conformation requires polymer statistics developed for the 3D case. Such a situation occurs in TEM when imaging a 3D specimen, or when the drying procedures yield polymers kinetically trapped onto a surface without subsequent options for relocation of initial contact points. A 2D chain statistical model as a basis for model development is the other extreme. This situation assumes an equilibrium conformation where the allowed fluctuations yield an excursion of the chain trajectory only parallel, and not perpendicular to the plane of the substrate. One can also imagine a situation in-between, where many points are quasi-adsorbed to the surface, while the

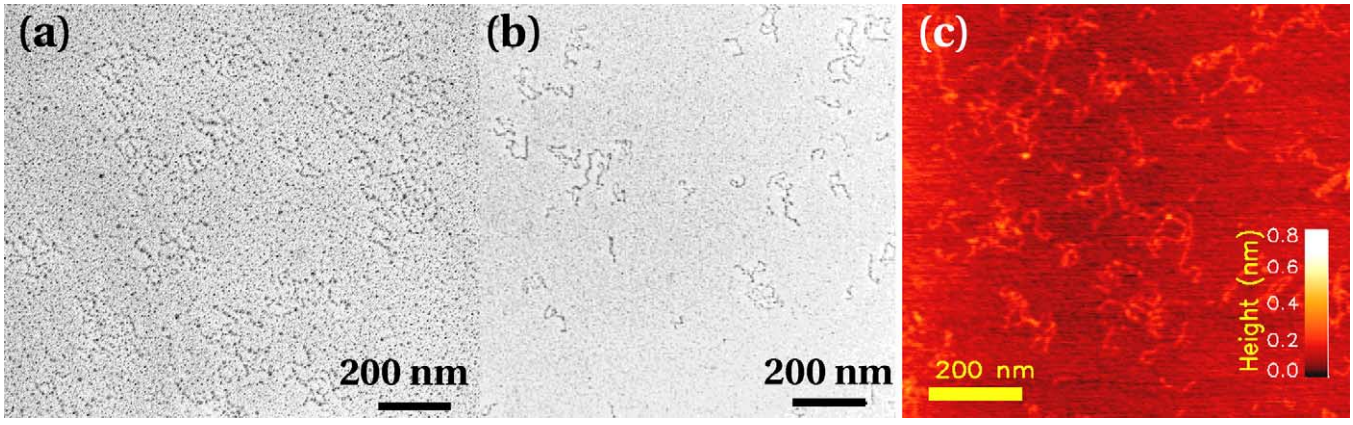

Fig. 4. Comparison of polysaccharide chain flexibility observed using TEM and AFM for polymers with different linkage patterns. Electron micrograph of bacterial exopolysaccharides produced by the halophilic Archaeon *Haloferax mediterranei* with mixed (1→6) and (1→4) linkages (a); Transmission electron micrograph of $sclerox_{1.0}$ which has a (1→3)-linked β-D-Glc*p* backbone (reproduced from Stokke et al.[33]) (b). Tapping mode AFM topograph of (1→4)-linked alginate (fraction of guluronic acid, $F_G = 0.66$) (c). The samples were prepared by vacuum drying of the polysaccharides dissolved in aqueous glycerol and followed by low-angle platinum rotary replication for the TEM studies.[33] Tapping mode AFM was carried out on the vacuum-dried specimens without the platinum replication.

remaining loops between these points are forced into the plane.[37,40]

The persistence length, L_p, can be determined from statistical analysis of the change in the tangent direction, θ, of the polymer chain as a function of segment separation, l, of the chain trajectory. The analysis assumes that the angle θ between consecutive segments can be described by a Gaussian distribution, that the interaction between the surface and the molecule does not alter the local chain rigidity, and that the observed two dimensional conformation is a 2D state as discussed above. Providing that these conditions are met, the following equations can be used for the analysis of the polymer chain flexibility using trajectories recorded from EM or AFM:[36]

$$\langle\theta(l)\rangle = 0 \quad (1)$$

$$\langle\theta^2(l)\rangle = l/L_p \quad (2)$$

$$\langle\cos(\theta(l))\rangle = e^{-l/2L_p} \quad (3)$$

$$\langle\theta^4(l)\rangle/\langle\theta^2(l)\rangle^2 = 3 \quad (4)$$

Here, the angle brackets denote the ensemble average of the variables. Eqs. (2) and (3) yield the basis for determination of L_p, whereas Eqs. (1) and (4) can be used to test if the underlying assumptions are satisfied.[36] In this way, Eqs. (1) and (4) provide necessary tests to verify that the data set is sufficiently uncorrelated, and thus validate the analysis.[37] Methods for excluding molecules aligned as e.g., a result of artefacts associated with the specimen preparation, has also been established and involved the use of an order parameter.[37] If such methods are not applied, alignment of polymer chains at the surface due to the substrate interactions or drying procedure, can be misinterpreted as an onset of excluded volume effects at chain lengths lower than what is observed in solution studies (the onset of the excluded volume effects being about $l \approx 30L_p$).

This approach has recently been applied to analyse conformations and flexibility of the bacterial polysaccharides xanthan[41] and succinoglycan,[42] including studies at different salt concentrations. We have previously given a review of some older data on polysaccharides using this framework.[43] In some of the latter reports, clear deviations from the assumption of the model described above are present. This fact could indicate that the molecules were not equilibrated at the surface, and could be one reason for the deviations reported between the groups.

Determination of the mean-square end-to-end distance offers an alternative route to provide information of chain stiffness,[37] but will not be detailed here due to the similarities, with regard to both concerns and possibilities, with the method based on Eqs. (1)–(4).

4.2. Determination of strandedness and co-existing structural morphologies of polysaccharides using EM and AFM

Ultramicroscopic imaging by EM and AFM provides information about individual molecules. This is at variance with most techniques for physical and chemical characterisation that yields a specified type of average. On the basis of images contour, lengths and end-to-end distances of individual molecules as well as distributions for a population of molecules can be obtained. If the molecular dimensions are known (mass per unit length), one can obtain molecular mass distributions from the contour length distributions. The mass per unit length, M_L, can be determined experimentally from the ratio of M_W/L_W or M_N/L_N. Comparing this with different models, gives an indication of the strandedness of the polymer, and the ratio can furthermore be compared to calculations based on the helical pitch (obtained from diffraction data) and the chemical structure. Analyses like these have been carried out to characterise the acetan-like extracellular polysaccharide produced by the *Acetobacter xylinum* strain CR1/4 under different growth conditions. In this study dimensional analysis together with static light scattering was used and the results indicated that the molecules formed double helices.[44] Additional examples include the bacterial polysaccharide xanthan, and fungal polysaccharides of the (1→3)-β-D-glucan family.

The values of M_L obtained for xanthan, $M_L = 2100 \pm 200$ g mol^{-1} nm^{-1}, indicate a double stranded nature. Direct visualisation of xanthan in the disordered state revealed co-existence of completely and partly strand-separated species and well-matched duplexes.[45,46] This important ability to image co-existing structural morphologies within an ensemble of polymers having the same chemical composition, is another important facet of ultramicroscopy that sets it apart from most other physical and chemical characterisation methods. Further examples include e.g., detection of co-existing circular and linear morphologies of scleroglucan following a de-renaturation cycle imposed by changing the solvent conditions and thereby the stability of the triple-helical state.[47–51] This approach can also be applied to determine cluster morphologies when capturing structural information in gelation of polysaccharides.[52,53] The detection of long-chain branches as reported for pectin,[54] is a further example of information that can be obtained from these techniques. Structural studies of carrageenan employing cryo-TEM, where the aqueous sample is ideally vitrified, show fibrous structures.[55] Although this study indicates that the electron optic contrast of single-polysaccharide chains is so low that they are hardly visible, the potential of this technique is expected to be large within e.g. gelation of bacterial polysaccharides such as gellan. Recent studies of col-

lapsed DNA showing a highly organised packing of the chains in a toroidal state,[56] indicate the potential of this approach.

4.3. Challenges and potentials of AFM imaging of polysaccharides

One advantage of AFM imaging as compared to TEM is the height information provided by the former. Ideally, the height measured by AFM should be comparable to the dimensions obtained from X-ray diffraction measurements of lateral packed polymer chains. However, due to a number of factors, AFM studies tend to measure height values lower than those determined with other experimental techniques. This is the case irrespective of whether the imaging process takes place in air under ambient conditions or in liquid. An influence from factors other than height variations producing additional topographic variation in the tip-specimen interaction cannot be ruled out. The differences in height are determined either from iso-force contours or positions with equal oscillation amplitudes of the AFM tip, in contact and non-contact mode, respectively. A residual water layer adsorbed onto the sample surface is expected to be of importance in influencing the measured topographic variations for imaging of dried specimens. This layer causes adhesion between the tip and the sample and may therefore affect the measured height. The thickness of this water layer will depend on both the hydrophobicity of the sample,[57] and on the relative humidity of the environment.[58,59] When imaging under liquid, electrostatic interactions between the tip and the sample, as well as between the tip and the mica, will have an influence on the measured height. These interactions will depend on the pH and ionic strength of the solution.[60] The height can thus be measured more accurately by choosing conditions in which charges on the sample and the tip are minimised. The second major obstacle in accurate height measurements comes from the fact that the AFM tip might cause compression of the sample during imaging.[61]

One example illustrating the potential of high-resolution studies using AFM is the report of direct imaging of helical repeats of acetan. AFM images revealed a periodicity in height along the chain, which was attributed to the helical structure of acetan.[62] Recently, there has been an improvement in AFM instrumentation that is reported to yield improved imaging of helical character in the case of DNA.[63] The rich plethora of helical structures reported for many bacterial polysaccharides represents a rich source of samples that wait to be studied by such techniques.

Imaging by AFM has still not reached its limitations. Improved lateral resolution is sought for mainly by employing sharper tips, and tips with carbon nanotubes attached. With their small diameter, carbon nanotube tips are expected to improve the lateral resolution during imaging.[64,65] Cantilevers smaller than the commercially available ones, having high resonance frequencies in liquid, allow for decreased acquisition time, to the order of a few seconds. This has been illustrated for DNA imaged employing a prototype AFM built for small cantilevers.[66] Moreover, it has also been shown that conventional silicon nitride cantilevers can be improved by focused ion beam milling to minimise the width of the cantilever legs, thus increasing their resonance frequencies in solution.[67] This is of interest, as increasing the acquisition rate will greatly increase the possibility of tracing molecular movement in time.

5. Single molecule force spectroscopy of bacterial polysaccharides

5.1. Single molecule force spectroscopy of bacterial polysaccharides

In the above analysis of polymer flexibility from chain trajectories, a Gaussian distribution of bending angles was assumed. In aqueous solution, thermal forces govern the dynamics and magnitudes of the bending angles. In addition to being an important imaging tool, AFM also offers the possibility to stretch single polymer chains and thereby probe their elasticity directly. This, and other nanomechanical testing devices, can be used to determine mechanical properties corresponding to conformations and deformations beyond those visited due to thermal energy.[68] The range of deformation forces where the free energy change is of entropic origin and deviations from this can be determined. The importance of enthalpic contributions to deformation free energies has been documented for a number of biopolymers within the DNA, proteins and polysaccharides classes. These studies also provided evidence that, at critical forces, many polysaccharides undergo force-induced conformational transitions, including e.g., deformation of the most stable ring conformation. Thus, this field of force spectroscopy offers fundamental new knowledge concerning the molecular origin of the deformation free energy of polysaccharide chains. Examples included here range from isolated well-defined components, to similar studies on the polysaccharide layer of microbial cells.

The first report of the use of the atomic force microscope to probe the elastic properties of a single polysaccharide chain was published in 1997.[69] In this study, carboxymethylated dextran chains labelled with streptavidin groups and chemically bound to a gold surface were brought in contact with AFM tips labelled with biotin. Upon retraction of the tip, single dextran polymers were stretched up to 250 pN, the maximum force supported by the biotin/streptavidin pair. To

explore the behaviour of the polysaccharide chain under forces exceeding 250 pN, a non-specific coupling based on the adsorption of the chain onto the AFM-tip was used. Up to a certain stretching force, entropic forces dominated the chain deformation. Above this force, the chain was forced into a stiffer conformation. The deformation curves were modelled by entropy springs with segment elasticity, and were also interpreted using molecular dynamics (MD) calculations. The elastic response was explained by a twist of the C-5–C-6 bond in the glucose unit, resulting in an elongation of the chain. At forces exceeding 250 pN, both simulations and measurements revealed a discontinuity of the deformation indicating a conformational change, which was also found to be reversible. The authors indicated that the transition might be caused by a flip of the dextran C-5–C-6 bond. In light of the more recent work of Marszalek et al. discussed below,[70] the nature of this transition might be related to the mechanically induced conformational change of the saccharide ring observed for polysaccharides with axial glycosidic bonds.

The studies on dextran were followed by similar studies on other polysaccharides: amylose, pullulan,[70] carboxymethylamylose, carboxymethylcellulose and heparin.[71] Using non-specific attachments to both surface and tip, polymers were stretched to forces up to several nN (Fig. 5). Sudden changes in the curvature of the force-elongation profile (Fig. 5) were identified as a nanomechanical fingerprint of α-(1→4)-linked polysaccharides, and disappeared when the pyranose rings were opened as a result of oxidation.[70] The pyranose ring was thus identified as the structural unit controlling the elasticity of the molecule, and the elastic behaviour of the α-(1→4)-linked polysaccharides was assumed to be caused by a force-induced deformation of the ring structure resulting in an elongation of the virtual bond vector. The overall transition was from a chair-like to a boat-like conformation. Force curves reflecting the stretching of molecules of different length indicated that the elastic properties scaled linearly with the chain length. The force at which the force-induced conformational transition occurred was constant for a polysaccharide with a certain structure, independent of the length of the polymer. The change in free energy, ΔG, per monomer associated with the conformational transition was estimated from the force spectra. It was 4.5 kcal mol^{-1} for the monomer units in amylose, and $\sim$11 kcal mol^{-1} for the monomers in dextran.[70] These energies are comparable to the calculated free energy of interconversion between conformers of cyclohexane and related six-membered rings, ranging up to 12 kcal mol^{-1} for the free monomers in solution.[72] Like cyclohexane, pyranose rings can adopt various conformations that can be described by variations in the ring dihedral angles, i.e., the chair, boat and twist-boat conformers. Due to the lack of symmetry introduced by the exocyclic substituents (i.e., the hydroxyl and hydroxymethyl groups) and the ring oxygen, glucopyranose exhibits more than one energetically and geometrically distinct form of the boat, twist-boat and chair conformers. The conformation and orientation of the pyranose ring observed in the AFM stretching experiments are not easily determined since different boat conformations of comparable energies can explain the observed elongation of the stretched polymer segment. The possible stretched conformation was investigated in a separate molecular dynamics simulation study of conformations.[73] Conformational deformation pathways in the form of potential curves starting from the ground-state chair conformation and ending at one of the boat or twist-boat structures were constructed. The twist-boat conformation was suggested as the most likely endpoint in the AFM experiment, but the existence of a hindrance for the transition to the twist-boat conformation, caused by geometrical constraints introduced by neighbouring monomers in the chain, could not be ruled out.

The conformational change was postulated to result from the torque generated by the axially oriented glycosidic bonds when a force was applied to the molecules. This interpretation implies that the glycosidic bonds act as mechanical levers, driving the conformational transitions of the pyranose ring. When the glycosidic bonds are equatorial the torque will be close to zero, causing no conformational change. This hypothesis predicts the number of transitions in a given pyranose monomer with a known ring conformation and linkage geometry. It has been investigated further in a study of polymers containing different numbers of axial linkages; two (pectin), one (amylose) or zero (methylcellulose).[74] The pyranose ring conformation was altered from a chair to a boat and then to an inverted chair in a clearly resolved two-step conversion in a study of the plant polysaccharide pectin (1→4-linked α-D-galacturonic acid, i.e., with two axial linkages, Fig. 5). With this work, the number of known force-driven transitions between the chair and boat conformers of the pyranose ring structure was expanded to include chair inversion. The authors expected the observed force-induced deformation of pyranose rings to play a role in accommodating mechanical stresses.

Single molecule force spectroscopy of xanthan using physical adsorption of xanthan to the AFM tip, revealed different mechanical properties of native and denatured xanthan, arising from different secondary structures.[75,76] A resemblance observed between the segment elasticity of denatured xanthan and dextran strengthened the hypothesis that the segment elasticity is due to the deforming of the monosaccharide unit within the polysaccharides. Force curves obtained when stretching double helical xanthan (Fig. 6) were different from the curves obtained for the polysaccharides described above.

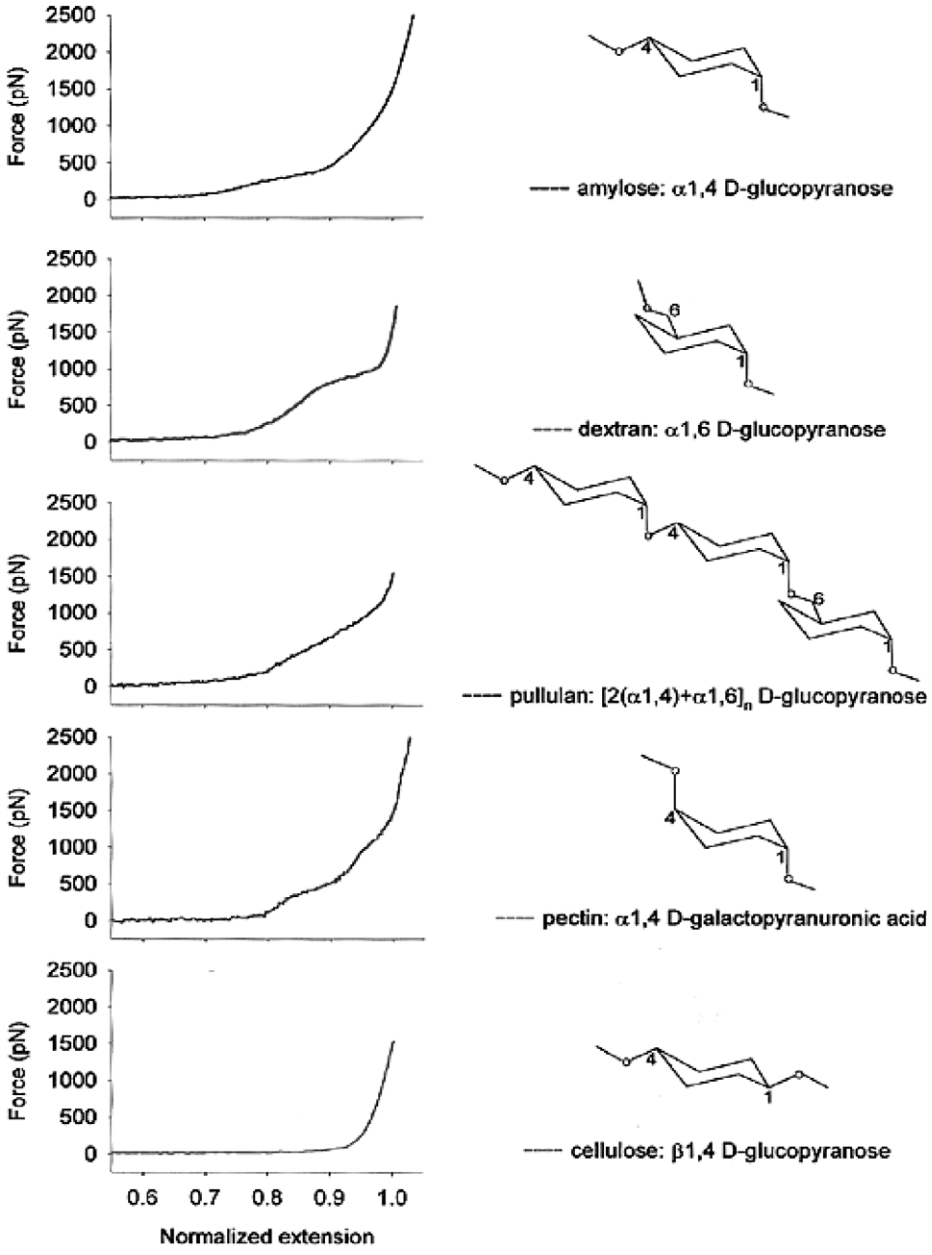

Fig. 5. Fingerprints of elasticity of linear polysaccharides obtained by AFM. Reproduced with permission from Marszalek et al.[79] On the left, force-extension relationships of single polysaccharides in solution obtained by vertically stretching the molecules between a substrate and an AFM cantilever. On the right, the (simplified) monomer and the type of glycosidic linkages in the polysaccharide for which the force-extension curves are displayed on the left. All force extension curves, except that of cellulose, display marked deviations from the purely entropic elasticity. These deviations are the "fingerprints" characteristic of monomers and linkages. All extensions were normalized by the molecule length determined at a force of 1500 pN.

A monotonic increase in force was seen, followed by a plateau, the height of which was the same in the collected force curves whereas its length varied. The force induced chain deformation was reversible up to the force marking the start of the plateau zone (400 pN). If the molecules were stretched beyond this force, the molecules would yield and a hysteresis was observed in the approach retract cycle. The observed connection between the double-helical conformation of xanthan and the plateau zone, together with the irreversible nature of the transition and the independence of the plateau force on the length of the stretched strand, made the authors attribute the plateau to the splitting of the helix. A force driven transition into a different helical structure similar to the overstretched state observed for B-DNA was also pointed out as a possible explanation

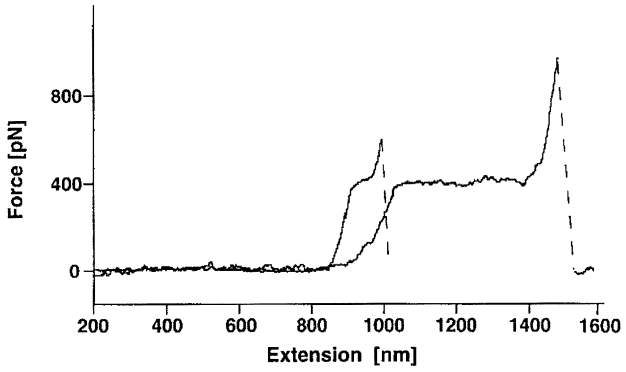

Fig. 6. Force-extension curve for native xanthan in PBS buffer. Reproduced with permission from Li et al.[75,76]

for the observed plateau in the curves. The tendency of xanthan to form aggregates, if exposed to certain thermal histories, has earlier been reported.[77] Investigations of the xanthan sample used[75,76] would therefore be of value in order to rule out the existence of such aggregates. The connection made between the observation of a plateau zone and the existence of a helix structure was strengthened by a later study on carrageenan, a non-bacterial polysaccharide.[78] Plateaus in the force curves were observed for carrageenan after adding NaI, a salt known to induce a coil-double helix transition in this polysaccharide. Such studies allow an experimental quantitative determination of the interactions stabilising e.g., a double-helical structure determined by X-ray fibre diffraction as discussed above.

Above, challenges and possible conventional routes for determination of the structure of polysaccharides were presented. Marszalek and co-workers suggested the use of single-molecule force spectroscopy as an alternative method for identifying the composition of polysaccharide samples by mechanically stretching individual molecules in solution. The results from the force-extension measurements discussed above are examples from a growing library of force curves suggested to be used as molecular fingerprints for identifying individual polysaccharides in complex mixtures (Fig. 5).[79] This novel AFM based techniques opens a possibility for mechanical testing of structure to function relations at the level of individual biological macromolecules. In such an approach, one should be aware that the obtainable data from stretching experiments are restricted to the linkage geometry, stretched segment length and persistence length of the polymers. The difficulty in determining the binding geometry will increase with increasing structural complexity of the polysaccharide. The reliability of a possible chemical identification based on force spectroscopy is judged to be, at this point, not on the level of the more established techniques used for primary structure determination. This is due to the rather limited variability of the force-elongation fingerprints relative to the possible chemical structure variation. In order to conclude about the exact chemical structure of polymers in an unknown sample, additional information must be obtained by other techniques. Other challenges that need to be addressed when studying the structure-function relation by single-molecule stretching experiments are related to the possible chemical heterogeneity and existence of impurities in the samples. In addition, polymers with a marked difference in chain stiffness, which will give rise to different force-distance curves, will also be distinguishable directly in images of the deposit, see e.g., the electron micrograph of xanthan blended with alginate.[43] On the other hand, force spectroscopy opens for identification of polymers attached to a surface, and therefore opens for studies affording additional information on localisation, as described below. Other phenomena, such as adhesion leading to force-extension profiles indicating a combination of desorption and stretching (Fig. 7), represent an additional type of information obtainable.

5.2. Single molecule force spectroscopy applied to study polysaccharides on the surface of bacteria

The methodology proposed by Marszalek and co-workers[79] not only facilitates the investigation of polysaccharide-extracts. As the surface of bacteria and cells are covered with polysaccharides, the technique opens for studies aimed at identifying and locating polysaccharides on cell surfaces. The first study where AFM was used in this respect, aimed at mapping the distribution of mannan polysaccharides on the surface of yeast cells.[80] The binding force was determined between concanavalin A and its corresponding polysaccharide ligand (a mannan) on the cell surface. Force maps were produced from the tip-surface force measured in a number of points within squares of 9 μm^2 on the surface. Molecular recognition events were identified on specific locations of the cell surface, reflecting a non-uniform distribution of mannan chains. A control experiment was carried out by determining the absence of adhesion between a bare gold-coated tip and the yeast cell surface. A repeated investigation of the same surface documented that the molecular recognition events could be reproduced to a large extent. This reproducibility of the force maps indicated that the probe was capable of identifying its target molecule on a heterogeneous surface.

The heterogeneity in bacterial surface macromolecules has also been investigated by bringing an AFM tip in contact with the surface of *Pseudomonas putida* cells and stretching the surface-polysaccharides.[81,82] Fitting the observations to the entropic freely jointed chain (FJC) model was suggested to reflect the presence of

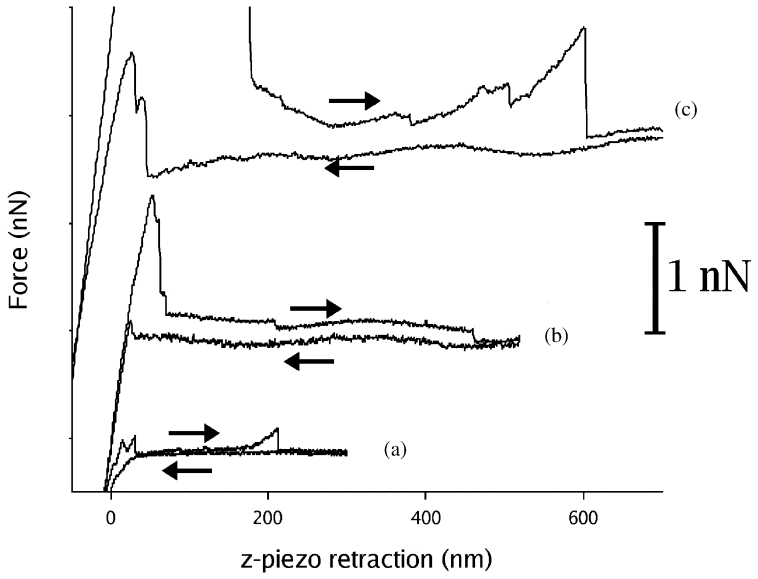

Fig. 7. Relations between force and z-piezo position (approach and retraction) for examples illustrating single polysaccharide stretching (a), polysaccharide desorption (b) and combined polysaccharide desorption and stretching (c). The actual examples were obtained as follow. (a) Stretching of mannuronan immobilised on the AFM tip and anchored with an epimerase enzyme to the mica support.[103] (b) Desorption between mannuronan anchored to the AFM tip and chitosan anchored to the mica substrate (in pH 6.4 MOPS buffer, 5 mM $CaCl_2$ and 5 mM NaCl). The desorption profile shows a ladder-like appearance where each plateau level reflects a distinct number of simultaneous mannuronan chains being desorbed. This is consistent with other reported polyelectrolyte desorption profiles.[104] (c) Force profiles between alginate anchored to the AFM tip and alginate on the surface (in pH 6.4 MOPS buffer, 5 mM $CaCl_2$ and 5 mM NaCl), showing simultaneous signatures of both desorption and polymer stretching.

molecules with different flexibility, and variability between different locations on the surface of a single cell appeared to be as important as cell-to-cell variability. The published data illustrate the need for increasing the control of the amount of interaction in such measurements. Ensuring that the stretching profile analysed is the result of a single polysaccharide chain being stretched between the AFM tip and the surface is essential in order to extract correct information. In AFM stretching experiments, information about the length of the polymer segment being stretched is inherent in the force curves. On the other hand, the force–z-piezo translation profile alone do not allow the determination of whether one or several polymers are contributing to the observations. Still, this kind of control is crucial since a situation where the force load between the tip and the surface is shared between two or several chains, will not reflect the properties of the single polymer chains. Efforts should therefore be made to reduce the probability for multiple unbinding events. The argument presented by Li et al.[75] that the small tip radius (20–50 nm) allow only a few molecules to interact with the tip is not in accordance with the observations presented by Camesano et al.,[81] showing several successive detachment events. Evans has proposed another approach to ensure a high probability for forming single molecular bonds. His strategy was based on adjusting the parameters in the experiments in order to observe a sufficiently infrequent bonding ($\sim$95% confidence for 1 attachment out of 10 trial touches).[83] The more infrequent the bonding, the higher the probability that the observations reflect the behaviour of single molecules.

AFM has also been used as a tool for measuring bacteria-surface interactions.[84] *E. coli* subjected to physiological stress synthesises and secretes capsular polysaccharides which, due to a high negative charge density, will prevent bacterial adhesion to surfaces. The effect of the surface polymers on the adhesion process was evaluated by comparing the interaction between AFM tips and lawns of *E. coli* strains with varying surface polysaccharide composition. Different experimental designs were tested; bacteria were immobilised onto a surface or onto cantilever tips. A combination of the two set-ups will allow studies of cell–cell binding events.

Although the study described above shows that the force between a bacterium and a surface can be probed by AFM, the interpretation of the force curves is difficult. According to Velegol et al.[85] the contributions of the polysaccharide layer to bacterium–surface interactions remain unresolved in the studies of Razatos,[84] as well as in similar studies.[86] This is due to an insufficient consideration of cell elasticity, which will make the bacterium deform under an applied load so that the

origin relative to the tip location is not known.[87] Other complicating factors also exist, such as electrostatics and the effect of glutaraldehyde cell-fixation on cell adhesion properties. Despite these limitations, polysaccharide fingerprinting and the use of chemically modified tips has allowed AFM to provide interesting observations at a molecular level on bacterial and other cell surfaces under near physiological conditions.

5.3. The use of single molecule force spectroscopy to study the involvement of polysaccharides in specific interactions

The days are gone when the role of the carbohydrate covering of cells was ascribed only to the protection of the cell against the outside environment by repulsive interactions. In a review on carbohydrate–carbohydrate interactions published in 1996 the authors stated that given the presence of carbohydrates on cell surfaces of all multicellular organisms as well as on pathogens from viruses to bacteria, the question should not be their involvement as such but their precise role in such encounters.[88] Cell-walls contain a gallery of carbohydrates and proteins that appear to interact with other molecules, both inside and outside the cell.[89] Oligosaccharides and glycoconjugates (glycoproteins and glycolipids) have intrigued biologists for decades as mediators of complex cellular events. This topic has recently been reviewed.[90] Less detail is known about the role of extracellular higher molecular mass carbohydrates.[91,92] In the following a few aspects of the role of polysaccharides in specific interactions are discussed with focus on some examples where AFM force spectroscopy has provided new information.

Misevic and co-workers were the first to provide, in an AFM study on marine sponges, quantitative evidence for the cohesive function of carbohydrates in recognition processes.[93,94] The self-adhesion system of aggregating cells involves membrane recognition. As a result of this system, cells discriminate between self and non-self.[95] Misevic and colleagues showed that an adhesion proteoglucan (AP) could be the primary cell adhesive molecule essential for the evolution of multicellularity. Observations of AP molecules by AFM showed that they are arranged as about 20 arms, 180 nm long, emanating from a common centre. The binding force between the AP of the marine sponge *Microciona prolifera* was quantified in various physiological conditions by linking the AP molecules to the AFM tip and to surfaces. Approach and retract cycles showed multiple steps on the retraction curve at distances ranging from 0 to 200 nm above the surface. The delayed interactions were interpreted as the result of interactions between the stringlike arms of the molecules. The magnitude of a single step, that is the interaction between two single arms, was 40 ± 15 pN. Both the probability of forming, and the strength of the AP–AP interactions, were reduced when reducing the calcium concentration, and monoclonal antibodies (mAb) were seen to inhibit the interaction, indicating that the adhesion forces measured by AFM originated from specific AP–AP interactions.

So far, there are to our knowledge no examples reported where single-molecule studies have shown a clear function of polysaccharides in biological interactions, but examples are known where further knowledge can be obtained using such techniques. One of these is a study on plant–pathogen interactions, where the final outcome of the interaction is propagated as a complex cascade of recognition, attack, and defence reactions at the host/microbe interface. Many signal molecules from the pathogen or from the host that are able to trigger defence responses are derived from polysaccharides naturally occurring during plant–microbe interactions.[96] Some species of algae are known to react by defence reactions to the presence of degradation products from their own cell walls.[97,98] It was suggested that the oligomers need to adopt an ordered single or double helix conformation for the biological recognition to take place. In plant–fungus systems, cell wall oligosaccharides from the host behave as signalling molecules and modulate the virulence of the pathogen. A certain sulfate substitution pattern of the host cell wall polysaccharide is needed to elicit the response.[99] In these systems, the detailed mechanism underlying the observed interactions is not known, and single-molecule force probes can be expected to advance the understanding of these systems.

6. Concluding remarks

Carbohydrates are not biologically inert molecules, but play active parts in cell-signalling processes by interactions with proteins and other carbohydrates. Despite the importance of carbohydrates in biology, the difficulty in studying carbohydrate–carbohydrate and carbohydrate–protein interactions has hindered efforts to develop an improved understanding of carbohydrate functions. This is due to the structural complexity of carbohydrates, coupled with the weak, often cation dependent and polyvalent character of carbohydrate–carbohydrate interactions and the weak binding affinities of carbohydrate–protein interactions. But even though difficult to study, polyvalent interactions have several mechanistic and functional advantages over their monovalent counterparts. Among these are the ability to produce graded responses with a single type of interaction, and the ability to increase the specificity of the interaction.[100] A cooperation between researchers in different fields is important in establishing the involvement of these interactions in biological processes and in

discovering new processes where carbohydrates play an active part. Ensemble studies by calorimetric or spectroscopic analyses of solutions do not provide direct information about binding forces between molecular pairs, and are thus complementary to AFM measurements. AFM based techniques might develop into becoming an important addition to the arsenal of analytical techniques used in carbohydrate research.

Acknowledgements

This work was supported by The Norwegian Research Council (grant numbers 145523/432, 134674/140, 145945/130, and 121894/420). We are indebted to Dr. A. I. Anton, Dept. of Biotechnology, University of Alicante, Spain for providing the archaeal polysaccharide.

References

1. Brant, D. A. *Curr. Opin. Struct. Biol.* **1999**, *9*, 556–562.
2. Sharon, N.; Lis, H. *Sci. Am.* **1993**, *268*, 74–81.
3. Talaga, P.; Vialle, S.; Moreau, M. *Vaccine* **2002**, *20*, 2474–2484.
4. Kocharova, N. A.; Perepelov, A. V.; Zatonsky, G. V.; Shashkov, A. S.; Knirel, Y. A.; Jansson, P.-E.; Weintraub, A. *Carbohydr. Res.* **2001**, *330*, 83–92.
5. Speiss, H. W. *Macromol. Chem. Phys.* **2003**, *204*, 340–346.
6. Brüll, L. P.; Huang, Z.; Thomas-Oates, J. E.; Paulsen, B. S.; Cohen, E. H.; Michaelsen, T. E. *J. Phycol.* **2000**, *36*, 871–881.
7. Dell, A.; Morris, H. R. *Science* **2001**, *291*, 2351–2356.
8. Gerwig, G. J.; Kamerling, J. P.; Vliegenthart, J. F. G. *Carbohydr. Res.* **1978**, *62*, 349–357.
9. Fraser, R. D. B.; MacRae, T. P. *Conformations in fibrous proteins*; Academic Press: New York, 1973.
10. Gessler, K.; Uson, I.; Takaha, T.; Krauss, N.; Smith, S. M.; Okada, S.; Sheldrick, G. M.; Saenger, W. *Proc. Natl. Acad. Sci. USA* **1999**, *96*, 4246–4251.
11. Rao, V. S. R. *Conformation of carbohydrates*; Harwood Academic Publishers: Amsterdam, 1998.
12. Veregin, R. P.; Fyfe, C. A.; Marchessault, R. H.; Taylor, M. G. *Carbohydr. Res.* **1987**, *160*, 41–56.
13. Stevensson, B.; Landersjö, C.; Widmalm, G.; Maliniak, A. *J. Am. Chem. Soc.* **2002**, *124*, 5946–5947.
14. Langan, P.; Nishiyama, Y.; Chanzy, H. *J. Am. Chem. Soc.* **1999**, *121*, 9940–9946.
15. Langan, P.; Forsyth, V. T.; Mahendrasingam, A.; Pigram, W. J.; Mason, S. A.; Fuller, W. *J. Biomol. Struct. Dyn.* **1992**, *10*, 489–503.
16. Nishiyama, Y.; Langan, P.; Chanzy, H. *J. Am. Chem. Soc.* **2002**, *124*, 9074–9082.
17. Shotton, M. W.; Pope, L. H.; Forsyth, T.; Langan, P.; Denny, R. C.; Giesen, U.; Dauvergne, M. T.; Fuller, W. *Biophys. Chem.* **1997**, *69*, 85–96.
18. Deri, A.; Cavatorta, F.; De Micheli, T.; Rupprecht, A.; Langan, P. *Physica B* **1997**, *234*, 215–216.
19. Atkins, E. D. T.; Nieduszynski, I. A.; Mackie, W.; Parker, K. D.; Smolko, E. E. *Biopolymers* **1973**, *12*, 1879–1887.
20. Grant, G. T.; Morris, E. R.; Rees, D. A.; Smith, P. J. C.; Thom, D. *FEBS Lett.* **1973**, *32*, 195–198.
21. Upstill, C.; Atkins, E. D. T.; Attwool, P. T. *Int. J. Biol. Macromol.* **1986**, *8*, 275–288.
22. Chandrasekaran, R.; Millane, R. P.; Arnott, S.; Atkins, E. D. T. *Carbohydr. Res.* **1988**, *175*, 1–15.
23. Viebke, C.; Borgström, J.; Piculell, L. *Carbohydr. Polym.* **1995**, *27*, 145–154.
24. Ikeda, S.; Morris, V. J.; Nishinari, K. *Biomacromolecules* **2001**, *2*, 1331–1337.
25. Gunning, A. P.; Kirby, A. R.; Ridout, M. J.; Brownsey, G. J.; Morris, V. J. *Macromolecules* **1996**, *29*, 6791–6796.
26. Chandrasekaran, R.; Radha, A.; Lee, E. J. *Carbohydr. Res.* **1994**, *252*, 183–207.
27. Crescenzi, V.; Dentini, M.; Dea, I. C. M. *Carbohydr. Res.* **1987**, *160*, 283–302.
28. Stokke, B. T.; Elgsaeter, A.; Kitamura, S. *Int. J. Biol. Macromol.* **1993**, *15*, 63–68.
29. Atkin, N.; Abeysekera, R. M.; Kronestedt-Robards, E. C.; Robards, A. W. *Biopolymers* **2000**, *54*, 195–210.
30. Hember, M. W. N.; Morris, E. R. *Carbohydr. Polym.* **1994**, *27*, 23–36.
31. Morris, E. R.; Gothard, M. G. E.; Hember, M. W. N.; Manning, C. E.; Robinson, G. *Carbohydr. Polym.* **1996**, *30*, 165–175.
32. Parolis, H.; Parolis, L. A. S.; Boan, I. F.; Rodriguez-Valera, F.; Widmalm, G.; Manca, M. C.; Jansson, P.-E.; Sutherland, I. W. *Carbohydr. Res.* **1996**, *295*, 147–156.
33. Stokke, B. T.; Falch, B. H.; Dentini, M. *Biopolymers* **2001**, *58*, 535–547.
34. Stokke, B. T.; Elgsaeter, A.; Skjåk-Bræk, G.; Smidsrød, O. *Carbohydr. Res.* **1987**, *160*, 13–18.
35. Tasker, S.; Matthijs, G.; Davies, M. C.; Roberts, C. J.; Schacht, E. H.; Tendler, S. J. B. *Langmuir* **1996**, *12*, 6436–6442.
36. Frontali, C.; Dore, E.; Ferrauto, A.; Gratton, E.; Bettini, A.; Pozzan, M. R.; Valdevit, E. *Biopolymers* **1979**, *18*, 1353–1373.
37. Stokke, B. T.; Brant, D. A. *Biopolymers* **1990**, *30*, 1161–1181.
38. Rivetti, C.; Guthold, M.; Bustamante, C. *J. Mol. Biol.* **1996**, *264*, 919–932.
39. Samori, P.; Ecker, C.; Gössl, I.; de Witte, P. A. J.; Cornelissen, J. J. L. M.; Metselaar, G. A.; Otten, M. B. J.; Rowan, A. E.; Nolte, R. J. M.; Rabe, J. P. *Macromolecules* **2002**, *35*, 5290–5294.
40. Joanicot, M.; Revet, B. *Biopolymers* **1987**, *26*, 315–326.
41. Camesano, T. A.; Wilkinson, K. J. *Biomacromolecules* **2001**, *2*, 1184–1191.
42. Balnois, E.; Stoll, S.; Wilkinson, K. J.; Buffle, J.; Rinaudo, M.; Milas, M. *Macromolecules* **2000**, *33*, 7440–7447.

43. Stokke, B. T.; Elgsaeter, A. *Micron* **1994**, *25*, 469–491.
44. Ridout, M. J.; Brownsey, G. J.; Gunning, A. P.; Morris, V. J. *Int. J. Biol. Macromol.* **1998**, *23*, 287–293.
45. Stokke, B. T.; Elgsaeter, A.; Smidsrød, O. *Int. J. Biol. Macromol.* **1986**, *8*, 217–225.
46. Stokke, B. T.; Smidsrød, O.; Elgsaeter, A. *Biopolymers* **1989**, *28*, 617–637.
47. Stokke, B. T.; Elgsaeter, A.; Brant, D. A.; Kitamura, S. *Macromolecules* **1991**, *24*, 6349–6351.
48. Stokke, B. T.; Elgsaeter, A.; Brant, D. A.; Kuge, T.; Kitamura, S. *Biopolymers* **1993**, *33*, 193–198.
49. Falch, B.; Elgsaeter, A.; Stokke, B. T. *Biopolymers* **1999**, *50*, 496–512.
50. McIntire, T. M.; Penner, R. M.; Brant, D. A. *Macromolecules* **1995**, *28*, 6375–6377.
51. McIntire, T. M.; Brant, D. A. *J. Am. Chem. Soc.* **1998**, *120*, 6909–6919.
52. Stokke, B. T.; Elgsaeter, A.; Kitamura, S. *Polym. Gels Netw.* **1994**, *2*, 173–190.
53. Hermansson, A.-M. *Carbohydr. Polymers* **1989**, *10*, 163–181.
54. Round, A. N.; MacDougall, A. J.; Ring, S. G.; Morris, V. J. *Carbohydr. Res.* **1997**, *303*, 251–253.
55. Borgstrom, J.; Piculell, L.; Viebke, C.; Talmon, Y. *Int. J. Biol. Macromol.* **1996**, *18*, 223–229.
56. Hud, N. V.; Downing, K. H. *Proc. Natl. Acad. Sci. USA* **2001**, *98*, 14925–14930.
57. Van Noort, S. J. T.; Van der Werf, K. O.; De Grooth, B. G.; Van Hulst, N. F.; Greve, J. *Ultramicroscopy* **1997**, *69*, 117–127.
58. Thundat, T.; Warmack, R. J.; Allison, D. P.; Bottomley, L. A.; Lourenco, A. J.; Ferrell, T. L. *J. Vac. Sci. Technol. A* **1992**, *10*, 630–635.
59. Ji, X.; Oh, J.; Dunker, A. K.; Hipps, K. W. *Ultramicroscopy* **1998**, *72*, 165–176.
60. Müller, D. J.; Engel, A. *Biophys. J.* **1997**, *73*, 1633–1644.
61. Weisenhorn, A. L.; Khorsandi, M.; Kasas, S.; Gotzos, V.; Butt, H.-J. *Nanotechnology* **1993**, *4*, 106–113.
62. Kirby, A. R.; Gunning, A. P.; Morris, V. J.; Ridout, M. J. *Biophys. J.* **1995**, *68*, 360–363.
63. Sugawara, Y. In *Noncontact atomic force microscopy*; Morita, S.; Wiesendanger, R.; Meyer, E., Eds. NC-AFM imaging of adsorbed molecules; Springer: Berlin, 2002; pp 183–192.
64. Dai, H.; Hafner, J. H.; Rinzler, A. G.; Colbert, D. T.; Smalley, R. E. *Nature* **1996**, *384*, 147–150.
65. Hafner, J. H.; Cheung, C.-L.; Wooley, A. T.; Lieber, C. M. *Prog. Biophys. Mol. Biol.* **2001**, *77*, 73–110.
66. Viani, M. B.; Schäffer, T. E.; Paloczi, G. T.; Pietrasanta, L. I.; Mith, B. L.; Thompson, J. B.; Richter, M.; Rief, M.; Gaub, H. E.; Plaxco, K. W.; Cleland, A. N.; Hansma, H. G.; Hansma, P. K. *Rev. Sci. Instrum.* **1999**, *70*, 4300–4303.
67. Hodges, A. R.; Bussmann, K. M.; Hoh, J. H. *Rev. Sci. Instrum.* **2001**, *72*, 3880–3883.
68. Strick, T. R.; Dessignes, M.-N.; Charvin, G.; Dekker, N. H.; Allemand, J.-F.; Bensimon, D.; Croquette, V. *Rep. Prog. Phys.* **2003**, *66*, 1–45.
69. Rief, M.; Oesterhelt, F.; Heymann, B.; Gaub, H. E. *Science* **1997**, *275*, 1295–1297.
70. Marszalek, P. E.; Oberhauser, A. F.; Pang, Y.-P.; Fernandez, J. M. *Nature* **1998**, *396*, 661–664.
71. Li, H.; Rief, M.; Oesterhelt, F.; Gaub, H. E.; Zhang, X.; Shen, J. *Chem. Phys. Lett.* **1999**, *305*, 197–201.
72. Pickett, H. M.; Strauss, H. L. *J. Am. Chem. Soc.* **1970**, *92*, 7281–7290.
73. O'Donoghue, P.; Luthey-Schulten, Z. A. *J. Phys. Chem. B* **2000**, *104*, 10398–10405.
74. Marszalek, P. E.; Pang, Y.-P.; Li, H.; Yazal, J. E.; Oberhauser, A. F.; Fernandez, J. M. *Proc. Natl. Acad. Sci. USA* **1999**, *96*, 7894–7898.
75. Li, H.; Rief, M.; Oesterhelt, F.; Gaub, H. E. *Adv. Mater.* **1998**, *3*, 316–319.
76. Li, H.; Rief, M.; Oesterhelt, F.; Gaub, H. E. *Appl. Phys. A Mater* **1999**, *68*, 407–410.
77. Stokke, B. T.; Foss, P.; Christensen, B. E.; Kierulf, C.; Sutherland, I. W. *Int. J. Biol. Macromol.* **1989**, *11*, 137–144.
78. Xu, Q.; Zou, S.; Zhang, W.; Zhang, X. *Macromol. Rap. Commun.* **2001**, *22*, 1163–1167.
79. Marszalek, P. E.; Li, H.; Fernandez, J. M. *Nat. Biotechnol.* **2001**, *19*, 258–262.
80. Gad, M.; Itoh, A.; Ikai, A. *Cell Biol. Int.* **1997**, *21*, 697–706.
81. Camesano, T. A.; Abu-Lail, N. I. *Biomacromolecules* **2002**, *3*, 661–667.
82. Abu-Lail, N. I.; Camesano, T. A. *Langmuir* **2002**, *18*, 4071–4081.
83. Evans, E. *Faraday Discuss.* **1998**, *111*, 1–16.
84. Razatos, A.; Ong, Y.; Sharma, M. M.; Georgiou, G. *J. Biomater. Sci. Polym. Ed.* **1998**, *9*, 1361–1373.
85. Velegol, S. B.; Logan, B. E. *Langmuir* **2002**, *18*, 5256–5262.
86. Camesano, T. A.; Logan, B. E. *Environ. Sci. Technol.* **2000**, *34*, 3354–3362.
87. Chan, D. Y. C.; Dagastine, R. R.; White, L. R. *J. Colloid Interface Sci.* **2001**, *236*, 141–154.
88. Spillmann, D.; Burger, M. M. *J. Cell. Biochem.* **1996**, *61*, 562–568.
89. Strauss, E. *Science* **1998**, *282*, 28–29.
90. Bertozzi, C. R.; Kiessling, L. L. *Science* **2001**, *291*, 2357–2364.
91. Sutherland, I. W. *Microbiology* **2001**, *147*, 3–9.
92. Sutherland, I. W. *Trends Microbiol.* **2001**, *9*, 222–227.
93. Dammer, U.; Popescu, O.; Wagner, P.; Anselmetti, D.; Günterodt, H.-J.; Misevic, G. N. *Science* **1995**, *267*, 1173–1175.
94. Misevic, G. N.; Burger, M. M. *J. Biol. Chem.* **1993**, *268*, 4922–4929.
95. Bozzaro, S.; Gerrisch, G. *J. Mol. Biol.* **1978**, *120*, 265–279.
96. Fritig, B.; Heitz, T.; Legrand, M. *Curr. Opin. Immunol.* **1998**, *10*, 16–22.
97. Küpper, F. C.; Kloareg, B.; Guern, G.; Potin, P. *Plant Physiol.* **2001**, *125*, 278–291.
98. Weinberger, F.; Richard, C.; Kloareg, B.; Kashman, Y.; Hoppe, H. G.; Friedlander, M. *J. Phycol.* **2001**, *37*, 418–426.
99. Bouarab, K.; Potin, P.; Correa, J.; Kloareg, B. *Plant Cell* **1999**, *11*, 1635–1650.

100. Mammen, M.; Choi, S. K.; Whitesides, G. M. *Angew. Chem. Int. Ed. Engl.* **1998**, *37*, 2754–2794.
101. Jansson, P.-E.; Lindberg, B.; Sandford, P. A. *Carbohydr. Res.* **1983**, *124*, 135–139.
102. Kuo, M.-S.; Mort, A. J.; Dell, A. *Carbohydr. Res.* **1986**, *156*, 173–187.
103. Sletmoen, M.; Skjåk-Bræk, G.; Stokke, B. T. **2003**, submitted.
104. Hugel, T.; Grosholz, M.; Claussen-Schaumann, H.; Pfau, A.; Gaub, H.; Seitz, M. *Macromolecules* **2001**, *34*, 1039–1047.